Trans Indian Inst Met (2019) 72(2):455–473
https://doi.org/10.1007/s12666-018-1496-4

TECHNICAL PAPER

Steady-State Materials and Enthalpy Balance: Applications to Ferroalloy Production and Industrial-Scale Validation

Ankur Agnihotri[1,2] · Prince K. Singh[1] · Rishikesh Mishra[1] · Dipak Mazumdar[1]

Received: 25 January 2018 / Accepted: 5 November 2018 / Published online: 22 November 2018

Abstract Steady-state material and enthalpy balance models for ferroalloy production in submerged arc furnace (SAF) have been developed. Two different types of ferroalloys, used commonly in the steel industry, namely high-carbon ferromanganese and high-carbon silicomanganese, were considered, and appropriate mass and energy conservation expressions were developed considering input, output and losses of various entities to/from two different 33 MVA SAFs. Several plant-specific parameters, such as material loss due to handling, off-gases, hot metal, slag and off-gas temperatures as well as heat losses from the SAFs, were incorporated in order to develop a predictive material and energy balance framework. Embodying types of feed materials, their composition and amount together with product composition along with relevant thermodynamic data, and amount of metal and slag produced in the two processes were estimated. Similarly, external power required to produce a given amount of ferroalloy was calculated by coupling material balance with an appropriate energy balance calculation scheme. It was demonstrated that estimates of hot metal production, slag generation and external electrical energy requirement were in reasonable agreement with industrial operating data. A graphical user interface was also developed to carry out material and energy balance calculations efficiently.

Keywords Ferroalloy production · Material and heat balance · Industrial-scale validation

List of symbols

$[a_{Mn}]$	Activity of manganese in the hot metal/ferroalloy (ferromanganese or silicomanganese)
(a_{MnO})	Activity of MnO in slag
D	Thermal demand per mole of product Mn (kJ/kg-mol Mn)
$E_{Ext.}$	External electrical energy supply per mole of Mn (kJ/kg-mol Mn)
H_{298}	Enthalpy at 1 atm. pressure and 298 K
H^{f}_{298}	Heat of formation at 298 K
$H_{1768,\underline{i}}$	Enthalpy content of dissolved species 'i' in a ferroalloy at 1768 K
L	Cooling losses per mole of product Mn (kJ/kg-mol Mn)
M_i	Wt% Mn or wt% Si in an ore 'i'
n^{g}_{CO}	Number of kg-moles of CO in the off-gas per kg-mole of product Mn
n^{g}_{CO}	Number of kg-moles of CO_2 in the off-gas per kg-mole of product Mn
n_{MgO}	Number of kg-moles of MgO per kg-mole of product Mn
n_{CaO}	Number of kg-moles of $CaCO_3$ per kg-mole of product Mn
n_{SiO_2}	Number of kg-moles of SiO_2 per kg-mole of product Mn
n_{MnO}	Number of kg-moles of MnO in slag per kg-mole of product Mn
n^{A}_{C}	Number of kg-moles of carbon (the active carbon) in the off-gas per kg-mole of product Mn

✉ Dipak Mazumdar
dipak@iitk.ac.in

[1] Department of Materials Science and Engineering, Indian Institute of Technology, Kanpur, India

[2] Present Address: Vardhman Special Steels Limited, Ludhiana, India

n_C^i	Number of kg-moles of carbon in the charge per kg-mole of Mn
p	Wt% Mn or wt% Si in hot metal
q	Wt% MnO or wt% SiO_2 in slag
S	Supply of enthalpy per kg-mole of product Mn (kJ/kg-mol Mn)
S	Wt% MnO in high-MnO slag generated during HCFeMn production
$W_{ore,i}$	Weight of ore i in the charge (kg)
W_{HMnO}	Weight of high-MnO slag (kg)
W_{slag}	Weight of slag generated during FeMn or SiMn production (kg)
W_{FeMn}	Weight of hot metal (ferromanganese) produced, kg
W_{SiMn}	Weight of hot metal (silicomanganese) produced (kg)
$(C/Mn)^{HM}$	Number of kg-moles of carbon per kg-mole of Mn in hot metal
$(Fe/Mn)^{HM}$	Number of kg-moles of Fe per kg-mole of Mn in hot metal
$(Si/Mn)^{HM}$	Number of kg-moles of silicon per kg-mole of Mn in hot metal
$(P/Mn)^{HM}$	Number of kg-moles of phosphorous per kg-mole of Mn in hot metal
γ_{MnO}	Activity coefficient of MnO in slag during ferromanganese production

1 Introduction

Large tonnage of ferroalloys such as FeMn, Fe–Si, SiMn, etc., are routinely used in steel industries as deoxidiser and alloying additions. These are typically produced in submerged electric arc furnace (SAF) through carbo-thermic reduction of manganese ore, silica, recycled slags, iron ore, etc. Simultaneous reduction of many impurity oxides present in ore, fuel and fluxing materials also takes place in the process contaminating final ferroalloys product. The presence of impurity elements in ferroalloys is known to adversely affect the efficiency of steelmaking. For example, sulphur present in FeSi as impurity is known to impair the efficacy of calcium injection in ladle metallurgy operations [1]. Therefore, low levels of impurities in ferroalloys are mandatorily prescribed to meet the present-day requirement of high-quality steelmaking. This has become more relevant in the context of production of high-manganese steels for high-end applications.

Nearly 2.7×10^3 kWh of electricity is required to produce a tonne of high-carbon ferromanganese, and this tends to make ferroalloy manufacturing energy-intensive and expensive. Rising costs of raw material and energy exert a considerable influence on the economics of steelmaking and are issues of concern. Accordingly, to assess process performance and efficiency of ferroalloy production in SAF, several investigations on thermodynamics [2], reductant selection [3], heat and material balance [4], etc., have been reported in the literature. A comprehensive treatise on production of manganese ferroalloys is also available in Ref. [5].

Material balance models rely on several empirical inputs such as composition, quantity, handling losses of different materials. Similarly, energy balance calculations, in addition to operating conditions (viz., heat loss), tend to overwhelmingly depend on thermochemical data such as heat of formation, dissolution, fusion, etc. In addition, various assumptions invoked to formulate such models influence their performance significantly. Given such, a priori assessment of material and energy balance models against production data assumes considerable significance and is warranted before they are implemented in audit and optimisation studies.

Consequently, the purpose of the present study is to develop appropriate material and energy balance models applicable to FeMn and SiMn production in submerged arc furnace. In the following sections, assumptions in modelling and formulation of models are first presented. Estimates of relevant material and energy balance parameters (viz., amount of ferroalloy produced and slag generated, amount of electricity consumed) are subsequently validated against operating data gathered from a month-long campaign in a domestic ferroalloy plant.

2 Brief Outline of Ferroalloy Manufacturing Techniques

2.1 Production of Ferromanganese

Commercial high-carbon ferromanganese is typically manufactured in submerged arc furnace. Feed stock typically includes carbonaceous materials (usually coke), manganese and iron ores as well as limestone and dolomite. Standard free energy of formation of manganese oxide indicates that the 'oxide-reductant (i.e. carbon) mixture' must be subjected to a high enough temperature in order to facilitate MnO → Mn conversion according to: $MnO(s) + C(s) \rightarrow [Mn] + \{CO\}$. Electrical power is used to drive the above reaction in the forward direction facilitating production of hot metal containing manganese.

Different types of oxides present in the ore, flux and fuel, having similar or lower stability than MnO or MnO_2, also undergo concurrent reduction in SAF. Extensive dissolution of carbon in the melt at high temperature finally results in the production of a ferroalloy containing

primarily Mn, Fe and C together with some S and P. The process also yields a slag containing predominantly MnO, CaO, MgO and SiO_2. A schematic of flow of different types of material and energy, to and from a SAF, during production of FeMn is illustrated in Fig. 1a.

2.2 Production of Silicomanganese

Production of silicomanganese in a SAF is essentially similar to that of FeMn. Silicomanganese is produced in submerged arc furnace by two different process routes, the main difference being the source of manganese in the charge materials. While one route uses solely the manganese ore, the other, in addition to the ore, uses high-manganese-oxide slag (MnO) produced during manufacturing of ferromanganese in SAF. This latter approach, known as the 'duplexing process', has been investigated in the present study.

Production of silicomanganese is relatively more energy-intensive as the strength of chemical bond between silicon and oxygen is relatively more than that between manganese and oxygen. A high enough temperature is therefore a prerequisite to ensure simultaneous reduction of SiO_2 and MnO. Several other oxides present in the ore, flux and fuel also undergo concurrent reduction at such elevated temperature. These together with carbon present in the charge material form a molten liquid (ferroalloy) in SAF containing primarily Mn, Si and C and other secondary elements such as S, P, etc. A slag containing CaO, MgO, SiO_2, etc., is also generated during the process. A schematic of the flow of different types of material and energy, to and from a SAF, during silicomanganese production is shown in Fig. 1b.

3 Present Work

3.1 Assumptions in Modelling

Material and energy balance models applicable to FeMn and SiMn production in submerged arc furnaces have been formulated assuming a steady-state operation. Consequently, input and generation of any element/compound in a SAF are assumed to be balanced by its output and losses. The following set of assumptions have been applied to formulate the models:

1. Composition and amount of raw materials entering SAF during batch production of FeMn and SiMn are known. These are known from chemical analysis as well as load cell data and are summarised in Tables 1 and 2, respectively.
2. Conservation equations are developed only for key elements present in hot metal and off-gas, such as Mn, Fe, Si, C, O etc. The presence of minor elements such as S, P, etc., is ignored.
3. Similarly, slag is primarily assumed to be composed of CaO, MnO, MgO, SiO_2 and Al_2O_3. Other possible oxides such as FeO are assumed to be present in the slag phase in negligible amount.
4. Total feed material loss (due to handling as well as in off-gases due to generation of dust and vapour) has been assumed to be fixed and taken to be equivalent to 8% of charge material. The value is specific to the plant and is arrived at from log sheet containing large amount of production data. It is important to mention here that in industrial-scale production of FeMn, $\sim$ 9% Mn loss in the exit gas has been reported.
5. Similarly, 93% of slag by total weight has been considered and remaining 7% has been assumed to be lost due to skull formation in runner and transport pits.

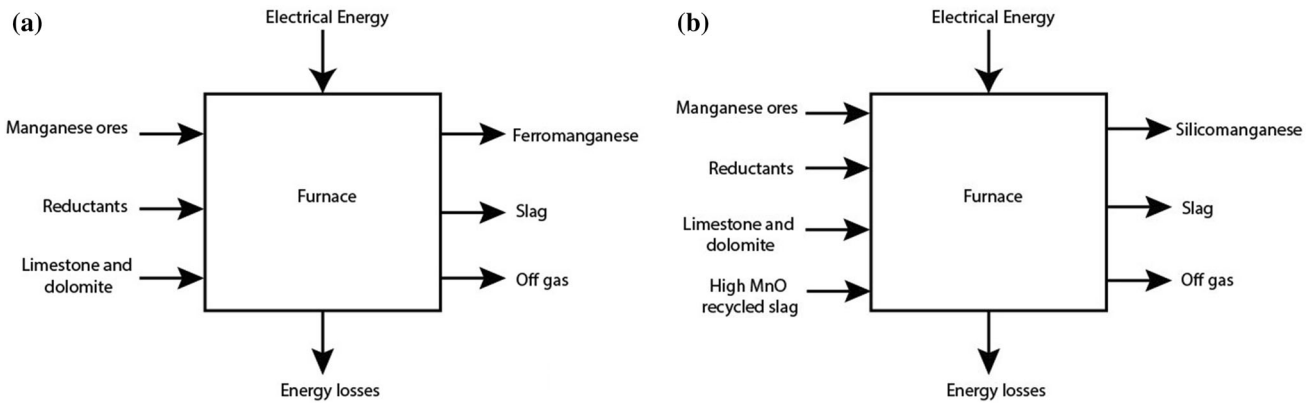

Fig. 1 Materials and energy flow into and from a submerged arc furnace. **a** Manufacturing of ferromanganese and **b** manufacturing of silicomanganese

Table 1 Data from a ferroalloy plant applied in the present work to develop and validate material and energy balance models for FeMn production

Chemical composition of metal			Chemical composition of slag				
Mn%	Si%	Phos%	MnO%	SiO_2%	CaO%	MgO%	Al_2O_3
(a) Composition and types of input material							
70.05	0.30	0.346	38.28	29.54	13.86	5.67	8.60
70.06	0.37	0.345	36.07	30.71	14.20	6.01	8.92
70.61	0.34	0.347	35.59	30.54	15.50	5.83	8.58
70.68	0.39	0.345	36.72	30.83	14.18	5.71	8.50
70.93	0.54	0.348	36.10	31.70	14.50	5.75	8.89
70.86	0.68	0.344	34.72	31.62	15.41	5.66	8.49
71.02	1.09	0.338	34.33	31.66	15.09	5.85	8.96
70.63	1.05	0.342	35.19	31.49	14.56	5.68	8.89
70.6	0.75	0.336	35.31	31.45	14.70	5.76	8.71
70.69	0.73	0.346	37.32	30.39	13.71	5.73	8.70

	Ore1	Ore2	Ore3	Ore4	Ore5	Ore6	Ore7	Coke	Dolomite	Dolomite	Lime stone, Jaisalmer	Iron ore
(b) Amount of feed material used												
Mn	48	43	44	47.5	47	32	30					
C								79				
Fe	5	6.5	7	6.5	6	24	26	1	1	1	1	62
SiO_2	12	13.5	12	10	14	5	5	15	8	4	4	5
Al_2O_3	3	3	3	3	3	4	4	4	15	15	15	4
CaO								2	32	32	48	
MgO								1	18	18	2	
Phos	0.1	0.26	0.21	0.16	0.2	0.05	0.05	0.14	0.01	0.01	0.01	0.05

Ore1 MT	Ore2 MT	Ore3 MT	Ore4 MT	Ore5 MT	Ore6 MT	Ore7 MT	Coke MT	Dolomite MT	Dolomite MT
(c) Amount of products (hot metal, slag and off-gas) generated									
114.5	104.5	57	34.2	47.5	76	0	87.40	5.32	34.58
120	110	60	36	50	80	0	94.00	5.60	36.40
146.5	107.25	29.25	35.1	48.75	0	78	91.65	5.46	35.49
153.5	112.75	30.75	36.9	51.25	0	82	96.35	5.74	37.31
146.5	107.25	29.25	35.1	48.75	0	78	91.65	5.46	35.49
146.5	107.25	29.25	35.1	48.75	0	78	91.65	5.46	35.49
143	104.5	28.5	34.2	47.5	0	76	89.30	5.32	34.58
146.5	107.25	29.25	35.1	48.75	0	78	90.00	5.46	35.49
139.5	101.75	27.75	33.3	46.25	0	74	85.10	5.18	33.67
136	99	27	32.4	45	0	72	82.80	5.04	32.76

Lime stone, Jaisalmer	Iron ore	Electrode paste	Shut off	Power	FeMn	Slag	Off-gas temp	Off-gas composition			
MT	MT	MT	Min	MWH	MT	MT	°C	O_2%	H_2%	CO_2%	CO%
(d) Amount of products (hot metal, slag and off-gas) generated											
13.30	2.60	2.85	40	454.2	166	124.5	217–318	1.0	1.0	38.0	44.0
14.00	0.00	2.80	0	490.0	179	134.3	190–302	1.5	0.7	37.0	45.0
13.65	0.00	3.20	0	492.2	180	135.0	210–302	1.0	1.4	37.0	48.0
14.35	0.00	3.25	0	493.0	181	135.8	190–303	1.2	1.0	37.0	52.0
13.65	0.00	3.20	35	477.0	174	130.5	165–265	1.7	0.4	41.0	52.0
13.65	3.30	3.60	14	479.2	175	131.3	142–220	1.5	1.8	41.0	54.0
13.30	5.45	3.20	0	493.4	180	135.0	152–220	1.5	1.0	42.0	52.0

Table 1 continued

Lime stone, Jaisalmer	Iron ore	Electrode paste	Shut off	Power	FeMn	Slag	Off-gas temp	Off-gas composition			
MT	MT	MT	Min	MWH	MT	MT	°C	O_2%	H_2%	CO_2%	CO%
13.65	5.85	3.50	17	484.4	177	132.8	150–218	1.6	1.0	38.0	50.0
12.95	1.20	3.20	130	447.8	153	122.3	166–273	1.8	1.0	35.0	47.0
12.60	3.60	3.45	17	481.0	176	132.0	260–290	2.0	0.9	38.0	48.0

6. Exit gas analysis, as shown in Tables 1 and 2, accounts for nearly 84–86% of the total gas composition. It is assumed that remaining 14–16% is inert (mainly nitrogen) and non-reacting in nature, but takes away sensible heat from the furnace since exit gases are discharged at $\sim$ 650 K.
7. Slag is assumed to be formed primarily due to chemical reaction between CaO and SiO_2. Other constituents such as MgO, MnO, etc., are assumed to be present in the slag. Their dissolution and the possibility of formation of complex oxides are not considered in this work since associated heat effects are found to be only marginal exerting no influence on the outcome from energy balance (see later).
8. To estimate thermal demand associated with ferroalloy production, measured slag and hot metal temperatures have been applied. Similarly, cooling water flow rates and corresponding temperature rise have been measured to quantify in situ thermal losses from the two SAFs.
9. Standard enthalpy and heat of formation of various elements/compounds as a function of temperature together with various thermophysical properties embodied in energy balance expressions are obtained from standard sources such as Refs. [2] and [6–8].
10. And finally, for the sake of convenience, energy balance expressions have been formulated on the basis of 'per kg-mole of product Mn' (synonymous to 'per kg-mole of Mn in hot metal or ferroalloy') rather than on corresponding mass basis. To this end, standard molar definition has been applied throughout the text, except that O rather than O_2 has been taken as a mole of oxygen. Approaches similar to those outlined by Peacey and Davenport [8] as well as Mazumdar [9] have been applied to formulate appropriate energy balance expressions.

Mass balance allows accounting for all the elements entered in the system and is based on the principle of conservation of mass. Looking from such a standpoint, energy and material balances are intricately interrelated. Consequently, accuracy of prediction from the latter tends to rely considerably on the accuracy of mass balance calculations. Therefore, a sequential calculation scheme, embodying material followed by energy balance, has been adopted in the present study. Adequacy of enthalpy data for different species in their applicable states' influences results from energy balance calculations. Consequently, sensitivity of calculations to specific values of thermochemical data has been studied prior to carrying out elaborate model predictions. Similarly, accuracy of feed and product analysis plays crucial roles and influences mass and energy balance calculations. Accordingly, chemical composition of ferroalloy and slag are also determined in parallel in the authors' laboratory (see Table 3) and assessed against equivalent plant data, reported, respectively, in Tables 1 and 2. As seen, the two sets of measurements complement each other reasonably well.

3.2 Production of Ferromanganese

3.2.1 Material Balance

Chemical composition and amount of ore, flux and carbonaceous material used to produce a given amount of ferromanganese (also termed as hot metal) and associated amounts of slag and off-gas are summarised in Table 1. Off-gas temperature needed to formulate energy conservation equations is also included in the table. Embodying feed characteristics and product chemistry, amount of slag generated during production of high-carbon ferromanganese can also be calculated considering conservation of lime (i.e. CaO), since entire amount of input lime, barring handling losses, is expected to be present in the slag phase. Lime or CaO is unlikely to dissociate in SAF, and hence calcium is unlikely an constituent of hot metal as the chemical analysis present in Table 1 indicates. Noting that there are different sources of CaO in input (viz., limestone,

Table 2 Data from a ferroalloy plant applied in the present work to develop and validate material and energy balance models for SiMn production

Species	Ore1	Ore2	Ore3	Ore4	Ore5	Ore6	Ore7	Sinter1	Sinter2	Ore8	Coke	Charcoal	Dolomite	Quartzite
(a) Composition and types of input material														
Mn	30.0	30.0	31.0	25.0	37.0	38.0	38	39.0	32.0	43.00	–	–	–	–
Fe	7.0	8.0	7.5	5.0	6.0	7.0	7.5	9.5	9.0	8.00	1.00	0.0	1.00	1.0
SiO_2	30.0	35.0	34.0	50.0	27.0	22.0	22	22.0	34.0	15.00	15.00	3.5	8.00	97.0
Al_2O_3	3.0	3.0	3.0	3.0	3.0	3.0	3	3.0	3.0	3.00	4.00	1.5	1.50	1.0
CaO	–	–	–	–	–	–	–	–	–	–	2.00		32.00	–
MgO	–	–	–	–	–	–	–	–	–	–	1.00		18.00	–
Phos	0.30	0.27	0.30	0.10	0.20	0.25	0.20	0.20	0.20	0.280	0.140	0.140	0.01	0.010
MnO	–	–	–	–	–	–	–	–	–	–	–	–	–	–
Fixed carbon	–	–	–	–	–	–	–	–	–	–	79.00	65.0	–	–

Chemical composition of metal				Chemical composition of slag				Off-gas composition			
Mn%	Si%	Phos%	MnO%	SiO_2%	CaO%	MgO%	Al_2O_3%	O_2%	H_2%	CO_2%	CO%
(b) Amount of feed material used											
61.66	15.42	0.335	15.76	46.18	13.93	7.09	12.41	1.0	4.9	9.0	66.0
61.85	15.35	0.346	15.68	46.26	14.04	7.25	12.27	2.0	2.7	12.0	60.0
			15.16	46.72	13.82	7.25	12.50	1.4	3.5	12.0	64.0
61.31	15.38	0.34	16.09	46.57	13.73	6.86	12.25	1.0	2.8	13.0	59.0
61.29	15.69	0.347	15.76	46.07	13.94	7.24	12.48	1.5	4.2	12.0	49.0
61.12	15.64	0.343	15.07	46.10	14.04	7.31	12.67	3.8	3.8	12.0	55.0
61.31	15.59	0.34	17.20	45.31	14.14	7.09	11.89	4.0	4.0	10.0	53.0
60.61	17.39	0.345	15.32	46.44	13.52	7.31	12.77	3.6	3.6	11.0	59.0
60.80	16.91	0.345	19.71	45.18	13.31	6.94	10.53	4.8	4.8	11.0	54.0
61.31	16.68	0.346	15.28	46.82	13.73	7.01	12.35	2.2	2.2	13.0	60.0
60.93	16.52	0.338	15.48	46.71	13.93	7.16	12.14	3.5	3.5	13.0	62.0
60.61	16.78	0.334	17.40	46.11	13.52	7.16	11.37	5.0	5.0	15.0	67.0
60.35	16.51	0.339	17.46	46.72	13.42	7.09	11.04	4.0	4.0	13.0	68.0
60.55	16.28	0.338	15.52	46.27	14.14	7.24	12.41	4.6	4.6	14.0	60.0
60.61	16.58	0.338	16.72	46.49	13.62	6.94	11.87	2.9	2.9	17.0	60.0
60.54	15.41	0.331	15.69	46.60	14.04	6.94	12.25	4.3	4.3	15.0	66.0
60.54	15.36	0.334	16.07	46.13	13.83	7.09	12.31	5.4	5.4	16.0	65.0
60.42	15.39	0.339	17.40	46.37	13.52	6.64	11.68	4.4	4.4	17.0	60.0
60.54	15.31	0.338	17.60	46.18	13.42	7.01	11.33	5.7	5.7	14.0	66.0
60.74	15.28	0.34	19.42	46.37	12.79	6.86	9.86	4.9	4.9	17.0	58.0

Day	Ore1 MT	Ore2 MT	Ore3 MT	Ore4 MT	Ore5 MT	Ore6 MT	Ore7 MT	Sinter1 MT	Sinter 2 MT	Ore8 MT	Coke MT
(c) Amount of products (hot metal slag and off-gas) generated											
1	66.00	0.00	0.00	0.00	0.00	42.00	0.00	24.00	0.00	44.40	57.40
2	0.00	0.00	27.50	0.00	0.00	17.50	0.00	10.00	0.00	18.50	24.00
3	0.00	0.00	52.25	0.00	0.00	29.00	0.00	27.50	0.00	30.90	47.30
4	0.00	0.00	46.75	0.00	0.00	25.50	0.00	25.50	0.00	26.00	42.50
5	0.00	0.00	35.75	0.00	0.00	19.50	0.00	19.50	0.00	19.50	32.50
6	0.00	0.00	0.00	0.00	0.00	0.00	0.00	0.00	0.00	0.00	0.00
7	0.00	0.00	55.00	0.00	0.00	30.00	0.00	30.00	0.00	30.00	49.25
8	0.00	0.00	55.00	0.00	0.00	30.00	0.00	30.00	0.00	30.00	47.70
9	0.00	0.00	57.75	0.00	0.00	27.25	0.00	35.75	0.00	29.80	49.35
10	0.00	0.00	67.25	0.00	0.00	30.75	0.00	26.25	8.00	35.00	54.05

Table 2 continued

Day	Ore1 MT	Ore2 MT	Ore3 MT	Ore4 MT	Ore5 MT	Ore6 MT	Ore7 MT	Sinter1 MT	Sinter 2 MT	Ore8 MT	Coke MT
11	0.00	0.00	84.50	0.00	0.00	39.00	0.00	0.00	26.00	45.50	61.10
12	0.00	0.00	84.25	7.00	0.00	39.60	0.00	0.00	27.00	40.30	65.30
13	0.00	0.00	63.00	10.50	0.00	31.50	0.00	0.00	21.00	28.35	51.45
14	0.00	0.00	72.00	12.00	0.00	36.00	0.00	0.00	24.00	30.40	58.80
15	0.00	0.00	69.00	11.50	0.00	34.50	0.00	0.00	23.00	28.75	57.50
16	0.00	0.00	75.00	12.50	0.00	37.50	0.00	0.00	25.00	31.25	62.50
17	0.00	0.00	69.00	11.50	0.00	34.50	0.00	0.00	23.00	28.75	57.50
18	0.00	0.00	72.00	12.00	0.00	36.00	0.00	24.00	0.00	27.90	60.00
19	0.00	0.00	37.80	6.30	0.00	18.90	0.00	12.60	0.00	14.49	31.50
20	0.00	0.00	64.20	10.70	0.00	32.10	0.00	21.40	0.00	24.61	53.50
21	0.00	0.00	69.00	11.50	34.50	0.00	0.00	23.00	0.00	26.45	57.50
22	0.00	0.00	69.00	11.50	34.50	0.00	0.00	23.00	0.00	26.45	57.50
23	0.00	0.00	72.00	12.00	36.00	0.00	0.00	24.00	0.00	27.60	60.00
24	0.00	66.00	0.00	11.00	33.00	0.00	0.00	22.00	0.00	25.30	55.00
25	0.00	72.00	0.00	12.00	0.00	36.00	0.00	24.00	0.00	27.60	60.00
26	0.00	75.00	0.00	12.50	0.00	37.50	0.00	25.00	0.00	28.75	62.50
27	0.00	72.00	0.00	12.00	0.00	36.00	0.00	29.00	0.00	24.60	60.00
28	0.00	72.00	0.00	12.00	0.00	0.00	36.00	25.00	0.00	24.00	60.00
29	0.00	47.00	0.00	23.00	0.00	0.00	20.90	28.25	0.00	26.50	50.00
30	0.00	38.00	0.00	27.60	0.00	0.00	15.20	28.50	0.00	28.50	47.50

Day	Charcoal MT	Dolomite MT	Quartzite MT	H MnO slag MT	Iron ore MT	El. paste MT	Shut off Min	Power MWH	SiMn MT	Slag MT	Off-gas temperature °C
1	10.00	6.00	14.40	96.00	14.40	2.95	17	469.0	110.0	93.50	251–320
2	4.00	2.50	6.00	40.00	6.00	3.45	497	209.0	48.00	40.80	235–290
3	5.05	4.75	10.55	76.00	12.25	1.55	0	379.0	89.00	75.65	297–350
4	4.25	4.25	9.35	68.50	12.25	2.10	237	336.4	79.00	67.15	302–367
5	3.25	3.25	7.15	52.00	9.75	2.25	480	272.2	63.00	53.55	260–333
6	0.00	0.00	0.00	0.00	0.00	0.00	915	46.0	10.00	8.50	55–110
7	5.00	5.00	11.00	80.00	15.00	0.80	7	355.4	83.00	70.55	189–336
8	5.00	5.00	11.00	80.00	15.00	2.20	7	406.0	95.00	80.75	264–346
9	5.25	5.25	13.25	84.00	16.60	2.55	35	436.0	102.00	86.70	242–355
10	5.75	5.75	12.95	92.00	18.00	2.95	65	467.0	110.00	93.50	290–348
11	6.50	6.50	10.40	104.00	19.50	3.00	0	496.0	117.00	99.45	293–350
12	6.75	1.00	11.50	113.75	19.75	3.05	0	498.0	117.00	99.45	275–334
13	5.25	0.00	9.45	89.25	13.65	2.85	90	459.4	108.00	91.80	302–348
14	6.00	0.00	8.80	102.00	17.60	3.10	0	494.0	116.00	98.60	298–350
15	5.75	0.00	8.05	97.75	14.95	3.40	20	484.6	114.00	96.90	293–348
16	6.25	0.00	8.75	106.25	16.25	2.80	0	495.8	116.00	98.60	295–355
17	5.75	0.00	8.05	97.75	14.95	3.05	0	495.0	116.00	98.60	315–356
18	6.00	0.00	10.50	102.00	17.70	2.85	0	499.2	117.00	99.45	290–340
19	3.15	0.00	5.67	53.55	9.45	3.00	412	286.0	66.00	56.10	173–333
20	5.35	0.00	9.63	90.95	16.05	0.90	77	447.2	104.00	88.40	173–374
21	5.75	0.00	10.35	97.75	17.25	2.80	180	408.6	95.00	80.75	329–370
22	5.75	0.00	10.35	97.75	16.55	2.75	37	472.6	111.00	94.35	320–360
23	6.00	0.00	10.80	102.00	15.60	3.35	7	493.8	116.00	98.60	332–356
24	5.50	0.00	8.00	93.50	16.20	3.20	177	425.4	99.00	84.15	336–344
25	6.00	0.00	8.40	102.00	18.00	1.70	7	492.4	115.00	97.75	264–350

Table 2 continued

Day	Charcoal MT	Dolomite MT	Quartzite MT	H MnO slag MT	Iron ore MT	El. paste MT	Shut off Min	Power MWH	SiMn MT	Slag MT	Off-gas temperature °C
26	6.25	0.00	8.75	106.25	18.75	2.95	0	495.6	116.00	98.60	284–376
27	6.00	0.00	8.40	102.00	18.00	2.55	0	498.4	117.00	99.45	282–350
28	6.00	0.00	8.40	102.00	18.00	2.90	10	460.5	108.00	91.80	292–348
29	5.00	0.00	5.70	85.00	15.65	2.80	30	387.5	90.00	76.50	315–368
30	4.75	0.00	8.05	80.75	13.25	1.80	7	429.0	100.00	85.00	266–336

Table 3 Key elements and their content in various industrial samples as tested at IIT Kanpur

S. no.	Sample	Element	Weight%
1	Slag no. 1	Carbon (C)	1.49
		Ferrous oxide (FeO)	1.83
2	Slag no. 2	Carbon (C)	0.19
		Ferrous oxide (FeO)	0.98
3	Silicomanganese	Carbon (C)	2.10
		Silicon (Si)	13.64
		Manganese (Mn)	62.45
		Iron (Fe)	19.45
4	High-C ferromanganese	Carbon (C)	6.65
		Manganese (Mn)	74.54
		Iron (Fe)	20.46

dolomite and coke), one can mathematically represent the conservation of lime via the following expressions:

$$\left(\sum_{i=1}^{n} W_i \times Y_i\right) = \left(W_{\text{slag}} \times X\right), \tag{1}$$

in which W_i is the weight of a fluxing agent i and Y_i is the corresponding wt% CaO. Similarly, W_{slag} is the weight of slag produced and X is the wt% CaO in slag (for explanation of symbols, refer to List of symbols).

Manganese enters SAF via different types of ore materials and manifests in the hot metal (as Mn) and in slag, *albeit* in a small amount, as MnO, indicated in Table 1. On the basis of the above, conservation of manganese can be mathematically expressed as:

$$\sum_{i=1}^{n} (W_{\text{ore},i} \times M_i) = (W_{\text{FeMn}} \times p) + (W_{\text{slag}} \times q), \tag{2}$$

in which M_i represents wt% Mn in ore i (= 55/87 * (wt% MnO_2 in ore i)) and q is the wt% Mn in slag (= 55/71 * (wt% MnO)).

Since compositions of ore and FeMn (i.e. M and p, respectively) are known and the amount of various ores ($W_{\text{ore},i}$) is given, consequently, amount of ferromanganese produced can be readily estimated from Eq. (2) embodying the amount of slag calculated via Eq. (1). As an alternative to Eqs. (1) and (2), an input-based, equivalent conservation equation for elemental manganese can also be written as:

$$\begin{aligned}\sum\nolimits_i (\text{weight of ore})_i\,(\text{kg}) \times \frac{55}{87 \times 100}(\text{wt\% MnO}_2 \text{ in ore})_i \\ = W_{\text{HM}} \times \frac{\text{wt\% Mn in ferromanganese}}{100} \\ + \left(\frac{56}{100}\right) \times \text{Total input weight of limestone} \\ \times \left(\frac{55}{71}\right) \times \frac{\text{wt\% MnO in slag}}{\text{wt\% CaO in slag}}.\end{aligned} \tag{3}$$

It is readily seen from Eq. (3) that embodying amount of various types of manganese ores, their composition as well as composition of hot metal from Table 1, weight of ferromanganese produced in each batch, W_{HM} can be readily estimated. Corresponding amount slag generated can be estimated from either Eq. (1) or Eq. (2).

3.2.2 Energy Balance

Energy balance expression has been formulated by adapting a demand–supply approach similar to the one advocated by Peacey and Davenport [8]. To this end, (a) thermal energy requirements (termed henceforth as demand) and (b) evolution of thermal energy (termed henceforth as supply) for various physico-chemical processes during production of FeMn are calculated separately for a unit kg-mole of Mn in hot metal. The thermal demand, D^{FeMn}, is formulated considering energy requirements for the following individual processes, for example,

1. breaking of the bond between Mn and O in MnO at room temperature and heating respective constituents to their desired temperatures, i.e. Mn to 1750 K (in hot metal) and O to 650 K (in the exit gas),
2. processes similar to (a) SiO_2, Fe_2O_3 and P_2O_5, since Si, Fe and P also undergo reduction in SAF to join the hot metal. Heat of mixing between Fe and Mn is ideal and therefore negligible, while dissolution of Si and P in ferromanganese at 1750 K is considered to be equivalent to their dissolution in a pure Fe melt,
3. breaking of H–O bond in moisture at 298 K, as free hydrogen is reported in the off-gas,
4. heating of coke from room temperature to 1750 K and its subsequent dissolution in liquid hot metal,
5. calcination of limestone and dolomite at 298 K,
6. heating of individual slag constituents (CaO, MgO, SiO_2, Al_2O_3 and MnO) from 298 K to slag-forming temperature, i.e. 1750 K, and the formation of primary slag assumed to be essentially $CaO{\cdot}SiO_2$. Chemical reactions and dissolution of other constituents such as MgO, Al_2O_3 and MnO in $CaO{\cdot}SiO_2$ are ignored since the associated enthalpy requirement for the dissolution process is typically small, and finally,
7. heating of all off-gas constituents (viz., CO, CO_2, N_2, O_2 and H_2) to 650 K.

Similarly, supply or release of chemical energy, S, in the process is due to various exothermic processes, namely

1. heat of formation of CO and CO_2 at 298 K and
2. heat of formation of $CaO{\cdot}SiO_2$ at 298 K.

In addition to demand (D^{FeMn}) and supply (S) of heat energy, inherent process losses (L) are also to be expected. Accordingly, under steady-state condition, the energy deficit, i.e. $D^{\mathrm{FeMn}} + L - S$, must be balanced by external supply of electricity. Embodying standard enthalpy and heat of formation notations [8, 9] (see list of symbols for explanation), energy demand term per unit kg-mole of Mn can be expressed as:

$$
\begin{aligned}
D^{\mathrm{FeMn}} = {} & 1.0\left(-H^{\mathrm{f}}_{298,\mathrm{MnO_2}}\right) + \left[H_{1750,\mathrm{Mn}} - H^{o}_{298,\mathrm{Mn}}\right] \\
& + \left(\frac{\mathrm{Si}}{\mathrm{Mn}}\right)^{\mathrm{HM}}\left(-H^{\mathrm{f}}_{298,\mathrm{SiO_2}}\right) + \left(\frac{\mathrm{Si}}{\mathrm{Mn}}\right)^{\mathrm{HM}}\left[H_{1750,\underline{\mathrm{Si}}} - H^{o}_{298,\mathrm{Si}}\right] \\
& + \frac{1}{2}\left(\frac{\mathrm{Fe}}{\mathrm{Mn}}\right)^{\mathrm{HM}}\left(-H^{\mathrm{f}}_{298,\mathrm{Fe_2O_3}}\right) + \left(\frac{\mathrm{Fe}}{\mathrm{Mn}}\right)^{\mathrm{HM}}\left[H^{o}_{1750,\mathrm{Fe}} - H^{o}_{298,\mathrm{Fe}}\right] \\
& + \left(\frac{C}{\mathrm{Mn}}\right)^{\mathrm{HM}}\left(H_{1750,\underline{\mathrm{C}}} - H^{o}_{298,\mathrm{C}}\right) + n^{\mathrm{A}}_{\mathrm{C}}\left(H^{o}_{650,\mathrm{C}} - H^{o}_{298,\mathrm{C}}\right) \\
& + \frac{1}{2}\left(\frac{\mathrm{P}}{\mathrm{Mn}}\right)^{\mathrm{HM}}\left(-H^{\mathrm{f}}_{298,\mathrm{P_2O_5}}\right) + \left(\frac{P}{\mathrm{Mn}}\right)^{\mathrm{HM}}\left[H_{1750,\underline{\mathrm{P}}} - H^{o}_{298,\mathrm{P}}\right] \\
& + (n_{\mathrm{CaO}})\left(-H^{\mathrm{f}}_{298,\mathrm{CaCO_3}}\right) + (n_{\mathrm{MgO}})\left(-H^{\mathrm{f}}_{298,\mathrm{MgCO_3}}\right) \\
& + (n_{\mathrm{H_2O}})\left(-H_{298,\mathrm{H_2O}}\right) \\
& + \left[1 + 3/4\left(\frac{\mathrm{Fe}}{\mathrm{Mn}}\right)^{\mathrm{HM}} + \left(\frac{\mathrm{Si}}{\mathrm{Mn}}\right)^{\mathrm{HM}} + \frac{5}{4}\left(\frac{\mathrm{P}}{\mathrm{Mn}}\right) + n^{\mathrm{g}}_{\mathrm{O_2}}\right] \\
& \left[H^{o}_{650,\mathrm{O_2}} - H^{o}_{298,\mathrm{O_2}}\right] + n_{N_2}\left(H^{o}_{650,\mathrm{N_2}} - H^{o}_{298,\mathrm{N_2}}\right) \\
& + n_{\mathrm{H_2}}\left(H^{o}_{650,\mathrm{H_2}} - H^{o}_{298,\mathrm{H_2}}\right) + n_{\mathrm{CaO}}\left[H^{o}_{1750,\mathrm{CaO}} - H^{o}_{298,\mathrm{CaO}}\right] \\
& + n_{\mathrm{SiO_2}}[H^{o}_{1750,\mathrm{SiO_2}} - H^{o}_{298,\mathrm{SiO_2}}] + n_{\mathrm{MgO}}[H^{o}_{1750,\mathrm{MgO}} - H^{o}_{298,\mathrm{MgO}}] \\
& + n_{\mathrm{Al_2O_3}}\left(H^{o}_{1750,\mathrm{Al_2O_3}} - H^{o}_{298,\mathrm{Al_2O_3}}\right) \\
& + n_{\mathrm{MnO}}\left[H^{o}_{1750,MnO} - H^{o}_{298,\mathrm{MnO}}\right] + n^{\mathrm{g}}_{\mathrm{CO}}\left(H^{o}_{650,\mathrm{CO}} - H^{o}_{298,\mathrm{CO}}\right) \\
& + n^{\mathrm{g}}_{\mathrm{CO_2}}\left(H^{o}_{650,\mathrm{CO_2}} - H^{o}_{298,\mathrm{CO_2}}\right).
\end{aligned}
\tag{4}
$$

In a similar manner, availability or supply of thermal energy per unit kg-mole of Mn can be represented as:

$$
\begin{aligned}
S = {} & n^{\mathrm{g}}_{\mathrm{CO}}\left(-H^{\mathrm{f}}_{298,\mathrm{CO}}\right) + n^{\mathrm{g}}_{\mathrm{CO_2}}\left(-H^{\mathrm{f}}_{298,\mathrm{CO_2}}\right) \\
& + n_{\mathrm{CaO}}\left(-H^{\mathrm{f}}_{298,\mathrm{CaO{\cdot}SiO_2}}\right).
\end{aligned}
\tag{5}
$$

In Eqs. (4) and (5), H^{o}_{T} and $H^{\mathrm{f}}_{\mathrm{T}}$, respectively, represent standard enthalpy and heat of formation evaluated at temperature, T. Similarly, $n^{\mathrm{A}}_{\mathrm{C}}$ and $\left(\frac{\mathrm{C}}{\mathrm{Mn}}\right)^{\mathrm{HM}}$, respectively, represent moles of carbon in the off-gas and hot metal (ferromanganese), which are together equivalent to n^{i}_{C}, moles of input carbon per kg-mole of manganese. In deriving Eq. (4), as a first approximation, thermal effects associated with dissolution of MnO, MgO and Al_2O_3 in slag and any subsequent complex oxide formation have been ignored, as these are found to contribute insignificantly to energy balance calculations. Furthermore, since the reported off-gas composition does not sum up to 100 (see Table 1), consequently, nitrogen as an inert gas is assumed to be present as the remainder in the exit gas (see Eq. 4). In order to estimate thermal demand effectively, as has been mentioned earlier, hot metal temperature during tapping of ferroalloy has been measured by a radiation pyrometer, over a duration of 300 s on several days, and therefrom, an average

Table 4 Hot metal temperature measured in the vicinity of tap-hole of the SAF 1

S. no.	Hot metal–slag temp. (°C)
1	1450
2	1449
3	1440
4	1473
5	1476
6	1468
7	1465
8	1475
9	1480
10	1476
11	1472
12	1468
13	1482
14	1435
15	1465
16	1467
17	1466

Average hot metal temperature = 1465 °C

representative temperature is estimated and applied to Eq. (4). It is to be mentioned here that slag and metal temperatures are assumed to be essentially identical and no attempt is therefore made to differentiate these. As a sample illustration, results of temperature measurements are presented in Table 4.

In formulating overall energy balance expressions, it is important to know the associated heat loss from the furnace. The shell of the submerged arc furnace is cooled by circulating water around its periphery. Therefore, at steady state, the rate of heat loss from the furnace can be considered to be equivalent to the heat removed by circulating water and approximated via the following rate expression:

$$\dot{Q}_{\text{Loss}} = \dot{m} C_{\text{P}} \Delta T, \tag{6}$$

in which $\dot{m}$ = mass flow rate of water (kg/s), C_{P} = specific heat of water (J/kg C), and ΔT = rise in water temperature (°C). If t_{on} (s) is the total duration over which power is supplied to the furnace in a day, energy loss per day is equivalent to $Q_{\text{Loss}} t_{\text{on}}$. During the same period, kg-moles of manganese produced are given by:

$$\text{n}_{\text{Mn}} = \frac{(W_{\text{HM}} \times [\text{wt\% Mn}])}{M_{\text{Mn}} \times 100}, \tag{7}$$

in which M_{Mn} is the atomic weight of manganese, and W_{HM} and [wt% Mn] are, respectively, the amount and grade of ferromanganese produced. Accordingly, batch-wise heat loss per kg-mole of manganese, L, is given by:

$$L = \left(\frac{\dot{Q}_{\text{Loss}} \times t_{\text{on}}}{n_{\text{Mn}}} \right). \tag{8}$$

Flow rate of water and corresponding rise in temperature of circulating water in the two SAFs engaged in the production of FeMn and SiMn are summarised in Table 5. On the basis of such and the total furnace operating time (see Tables 1, 2) as well as the amount of hot metal produced, heat loss (L) per kg-mole of manganese can be conveniently estimated. It is to be noted here that heat loss from the two SAFs are found to be typically small and approximately 10% of the total electrical energy supplied. In addition to heat removed via circulating water, some additional heat loss is expected, since such furnaces are rarely completely leak proof. Due to hazards of high-temperature measurements and plant logistics, such losses can not be accounted for in the present work.

On the basis of the above, the required external electrical energy supplied, $E_{\text{ext.}}^{\text{FeMn}}$, per kg-mole of Mn produced, can be related to D^{FeMn}, L and S as:

$$E_{\text{ext.}}^{\text{FeMn}} = D^{\text{FeMn}} + L - S. \tag{9}$$

Thus, given the operating data as well as material and energy balance models, respective estimates of demand (D^{FeMn}), loss (L) and supply (S) can be made and the corresponding energy deficit in the process, per kg-mole of manganese produced, can be deduced via Eq. (9).

Operating data, such as daily power consumption, the duration of furnace operation and the total amount of hot metal produced, are routinely recorded in ferroalloy production unit. However, Tables 1 and 2 show the power consumption in MWh on a daily basis. Prior to any comparison with estimated values, the reported power supply in MWh must first be converted to appropriate unit (e.g. kJ/kg mol of Mn).

Thus, if Z is the daily power consumption in MWh to produce a given amount of hot metal, W_{HM}, equivalent electrical energy (E) consumed is: $Z \times 3600 \times 1000$ kJ. Since equivalent kg-moles of Mn produced is: $\left(W_{\text{HM (k)}} \times \frac{[\text{wt\%Mn}]}{100} \right) / M_{\text{Mn}}$, consequently, actual external electrical energy supply per kg-mol of Mn can be expressed as:

$$E_{\text{ext.}}^{\text{FeMn}} \,(\text{kJ/kg - mol of Mn}) = \frac{Z \times M_{\text{Mn}} \times 36 \times 10^7}{[\text{wt\% Mn}] \times \text{W}_{\text{HM}}\,(\text{kg})}, \tag{10}$$

in which Z is the power in MWh required to produce W_{HM} kg of ferromanganese. Actual energy supply deduced via Eq. (10) can now be compared with the corresponding energy deficit estimated from Eq. (9) to demonstrate the adequacy of material and energy balance calculations.

Table 5 Cooling water flow rate and rise in water temperature in the two submerged arc furnaces

Number of measurements	Inlet temp. (°C)	Outlet temp. (°C)	Temp. difference (°C)	Water flow rate (m^3/h)
(a) SAF 1				
1	30.2	35.5	5.3	46.2
2	30.0	36.5	6.5	46.27
3	31.0	36.0	5.0	46.2
4	30.0	35.0	5.0	46.2
5	30.0	35.0	5.0	46.2
6	30.5	35.5	5.0	46.2
7	30.5	35.5	5.0	46.2
8	31.0	35.0	4.0	46.2
9	30.5	36.0	5.5	46.2
10	30.0	35.5	5.5	46.2
(b) SAF 2				
1	31.0	35.0	4.0	51.3
2	31.0	35.0	4.0	51.3
3	31.0	35.5	4.5	51.3
4	30.5	35.0	4.5	51.3
5	31.0	36.0	5.0	51.3
6	31.0	35.0	4.0	51.3
7	31.0	35.0	4.0	51.3
8	31.5	35.0	4.5	51.3
9	31.0	35.5	4.5	51.3
10	31.0	35.0	4.0	51.3

3.3 Production of Silicomanganese

3.3.1 Material Balance

Composition and amount of charge materials such as ores, fluxes and fuels used in the production of SiMn are presented in Table 2. From the given amount and composition of charge materials as well as composition of slag and hot metal, amounts of slag generated as well as of SiMn produced can be readily calculated following a procedure outlined already in the preceding section. This is therefore not reiterated here. During the production of silicomanganese, SiO_2 is used as the source of Si, while different types of manganese ores as well as high-MnO slag generated during HCFeMn production are used as the source of manganese. Amount of SiMn produced in the process can be addressed from the standpoint of conservation of either manganese or silicon. Following the procedure presented in Sect. 3.2.1, manganese and silicon balance expressions under steady state can be, respectively, represented as:

$$\sum_{i=1}^{n}(W_{\mathrm{Ore},i}\times M_i)+\left(\frac{55}{71}\times s\times W_{\mathrm{HMnO}}\right)=(W_{\mathrm{SiMn}}\times p)+\left(\frac{55}{71}\times W_{\mathrm{slag}}\times q\right) \tag{11}$$

and

$$\sum_{i=1}^{n}\left(\frac{28}{60}\times W_{\mathrm{Ore},i}\times M_i\right)=(W_{\mathrm{SiMn}}\times p)+\left(\frac{28}{60}\times W_{\mathrm{Slag}}\times q\right), \tag{12}$$

in which $W_{\mathrm{Ore},i}$ = weight of ore i, W_{HMnO} = weight of high-MnO slag used as an additional source of manganese, W_{slag} = weight of slag generated during SiMn production, W_{SiMn} = weight of hot metal (i.e. SiMn) produced (all in SI unit), M_i = wt% Mn or Si in ore i, p = wt% Mn or Si in hot metal, q = wt% MnO or SiO_2 in slag generated, and s = wt% MnO in the high-MnO slag.

Either of the two equations, as pointed out already, can be applied to calculate the amount of silicomanganese produced. Since the concentration of Mn in silicomanganese is relatively higher, therefore for better accuracy, conservation equation for manganese (e.g. Eq. 11) has been applied to

estimate the amount of SiMn produced. The embodying amount and composition of different charge materials as well as composition of the hot metal and slag can be seen from Table 2. The amount of slag generated is first calculated from an equation similar to Eq. (1) presented earlier. Following such, the corresponding amount of hot metal (SiMn) produced is estimated via Eq. (11).

3.3.2 Energy Balance

Energy balance expression for production of SiMn has been formulated following essentially the same procedure outlined in Sect. 3.2.2. Accordingly, thermal energy demand per kg-mole of Mn present in SiMn has been represented as:

$$\begin{aligned} D^{\mathrm{SiMn}} &= 0.82\left(-H^{\mathrm{f}}_{298,\mathrm{MnO_2}}\right) + 0.18\left(-H^{\mathrm{f}}_{298,\mathrm{MnO}}\right) \\ &+ \left[H_{1750,\mathrm{Mn}} - H^{o}_{298,\mathrm{Mn}}\right] + \left(\frac{\mathrm{Si}}{\mathrm{Mn}}\right)^{\mathrm{HM}}\left(-H^{\mathrm{f}}_{298,\mathrm{SiO_2}}\right) \\ &+ \left(\frac{\mathrm{Si}}{\mathrm{Mn}}\right)^{\mathrm{HM}}\left[H_{1750,\underline{\mathrm{Si}}} - H^{o}_{298,\mathrm{Si}}\right] \\ &+ \frac{1}{2}\left(\frac{\mathrm{Fe}}{\mathrm{Mn}}\right)^{\mathrm{HM}}\left(-H^{\mathrm{f}}_{298,\mathrm{Fe_2O_3}}\right) + \left(\frac{\mathrm{Fe}}{\mathrm{Mn}}\right)^{\mathrm{HM}}\left[H_{1750,\mathrm{Fe}} - H^{o}_{298,\mathrm{Fe}}\right] \\ &+ \left(\frac{\mathrm{C}}{\mathrm{Mn}}\right)^{\mathrm{HM}}\left(H_{1750,\underline{\mathrm{C}}} - H^{o}_{298,\mathrm{C}}\right) + n^{\mathrm{A}}_{\mathrm{C}}\left(H^{o}_{650,C} - H^{o}_{298,\mathrm{C}}\right) \\ &+ \frac{1}{2}\left(\frac{\mathrm{P}}{\mathrm{Mn}}\right)^{\mathrm{HM}}\left(-H^{\mathrm{f}}_{298,\mathrm{P_2O_5}}\right) + \left(\frac{\mathrm{P}}{\mathrm{Mn}}\right)^{\mathrm{HM}}\left[H_{1750,\underline{\mathrm{P}}} - H^{o}_{298,\mathrm{P}}\right] \\ &+ (n_{\mathrm{CaO}})\left(-H^{\mathrm{f}}_{298,\mathrm{CaCO_3}}\right) + (n_{\mathrm{MgO}})\left(-H^{\mathrm{f}}_{298,\mathrm{MgCO_3}}\right) \\ &+ (n_{\mathrm{H_2O}})\left(-H_{298,\mathrm{H_2O}}\right) \\ &+ \left[0.91 + 3/4\left(\frac{\mathrm{Fe}}{\mathrm{Mn}}\right)^{\mathrm{HM}} + \left(\frac{\mathrm{Si}}{\mathrm{Mn}}\right)^{\mathrm{HM}} + \frac{5}{4}\left(\frac{\mathrm{P}}{\mathrm{Mn}}\right)^{\mathrm{HM}} + n^{\mathrm{g}}_{\mathrm{O_2}}\right] \\ &\left[H^{o}_{650,\mathrm{O_2}} - H^{o}_{298,\mathrm{O_2}}\right] + n_{\mathrm{N_2}}\left(H^{o}_{650,\mathrm{N_2}} - H^{o}_{298,\mathrm{N_2}}\right) \\ &+ n_{\mathrm{H_2}}\left(H^{o}_{650,\mathrm{H_2}} - H^{o}_{298,\mathrm{H_2}}\right) + n_{\mathrm{CaO}}\left[H^{o}_{1750,\mathrm{CaO}} - H^{o}_{298,\mathrm{CaO}}\right] \\ &+ n_{\mathrm{SiO_2}}\left[H^{o}_{1750,\mathrm{SiO_2}} - H^{o}_{298,\mathrm{SiO_2}}\right] \\ &+ n_{\mathrm{MgO}}[H^{o}_{1750,\mathrm{MgO}} - H^{o}_{298,\mathrm{MgO}}] + n_{\mathrm{Al_2O_3}}\left(H^{o}_{1750,\mathrm{Al_2O_3}} - H^{o}_{298,\mathrm{Al_2O_3}}\right) \\ &+ n_{\mathrm{MnO}}[H^{o}_{1750,\mathrm{MnO}} - H^{o}_{298,\mathrm{MnO}}] + n^{g}_{\mathrm{CO}}(H^{o}_{650,\mathrm{CO}} - H^{o}_{298,\mathrm{CO}}) \\ &+ n^{g}_{\mathrm{CO_2}}\left(H^{o}_{650,\mathrm{CO_2}} - H^{o}_{298,\mathrm{CO_2}}\right). \end{aligned} \tag{13}$$

It is important to mention here that the only difference between Eqs. (4) and (13) is the representation of heat of formation terms associated with manganese oxides. In ferromanganese production, while entire manganese is obtained from MnO_2 ores, during silicomanganese production, as per industrial practice, 82% of manganese is derived from MnO_2 ore, while the remainder from the high-MnO slag generated during ferromanganese production. Thus, in lieu of $(-H^{\mathrm{f}}_{298,\mathrm{MnO_2}})$ in Eq. (4), 0.82 $(-H^{\mathrm{f}}_{298,\mathrm{MnO_2}})$ and 0.18 $(-H^{\mathrm{f}}_{298,\mathrm{MnO}})$ are used in Eq. (13). The factors 0.82 and 0.18, as one would note here, conform to the actual plant practice and are specified by the ferroalloy producer. Similarly, Eq. (5) holds good for SiMn production as well, and therefore, chemical energy generated in the process can be represented as:

$$\begin{aligned} S = {} & n^{\mathrm{g}}_{\mathrm{CO}}\left(-H^{\mathrm{f}}_{298,\mathrm{CO}}\right) + n^{\mathrm{g}}_{\mathrm{CO_2}}\left(-H^{\mathrm{f}}_{298,\mathrm{CO_2}}\right) \\ & + n_{\mathrm{CaO}}\left(-H^{\mathrm{f}}_{298,\mathrm{CaO\cdot SiO_2}}\right). \end{aligned} \tag{14}$$

On the basis of preceding discussion and operating data presented in Tables 2 and 4, respectively, $E^{\mathrm{SiMn}}_{\mathrm{Ext}}$, relevant to silicomanganese production, has been calculated following procedures outlined in Sect. 3.2.2.

3.4 The Graphical User Interface

To efficiently perform material and energy balance calculations, a Java™ based graphical user interface (GUI) has been developed. In this, two distinct modules, one each for mass and energy conservations has been created, allowing sequential, user-driven solution of mass and energy balance equations. Provisions have been made in the GUI to compare numerical estimates with corresponding industrial-scale data so as to assess visually the general adequacy of the procedure developed.

The mass balance module has been designed to take input of relevant industrial data, such as composition and amount of various charge materials, composition of hot metal and slag, etc., needed to perform calculations and to derive estimates of (a) weight of hot metal produced and (b) weight of slag generated through solution of respective mass conservation equations. This also allows calculation of several technologically relevant parameters, such as % yield, amount of various feed materials per tonne of hot metal produced, etc.

Following such, (a) thermal energy demand (D), (b) thermal energy supply (L) and (c) energy losses (L) are estimated in three separate submodules, incorporating thermochemical and operating data as well as output from the material balance module. On the basis of such, batch-specific electrical energy requirement is calculated. As a sample illustration, one of the panels of the GUI, relevant to material balance calculations, is shown in Fig. 2.

4 Results and Discussion

Comparisons between estimated (via Eqs. 1, 2) and actual (Table 1) amounts of ferromanganese produced and slag generated are illustrated in Fig. 3a, b, respectively. As seen, the actual or reported amounts of slag and ferromanganese are in reasonable agreement with the corresponding calculated values. The difference between the

two can be taken as insignificant given that the calculations are based on empirically determined weight, composition, etc., which are prone to error and uncertainty. Estimates of hot metal shown in Fig. 3b, as one would note here, have been derived assuming 8% loss of charge material due to handling, loss of volatile matter and moisture, etc., as pointed out already. This can be consistently applied in all material balance calculations reported in this work. Similarly, the reported weights of slag presented in Tables 1 and 2, which are used as a basis of comparison, are 93% of the actual amount of slag produced, since drainage of slag, accumulation/holding and weighing processes together account for about 7% loss.

Assessment of the efficiency of FeMn production in the 33 MVA SAF can be carried out by considering slag–metal–gas equilibrium (viz., MnO–Mn–C–CO) system at 1738 K and 1 atm. total pressure. Therefore, reduction of manganese oxide by solid carbon is represented via the following chemical reaction:

$$(\mathrm{MnO}) + \mathrm{C(s)} = [\mathrm{Mn}] + \mathrm{CO(g)} \tag{15}$$

The equilibrium constant for the above reaction is:

$$K_{\mathrm{eq}} = \frac{[a_{\mathrm{Mn}}] \times p_{\mathrm{CO}}}{(a_{\mathrm{MnO}}) \times a_{\mathrm{c}}} \tag{16}$$

or, alternatively,

$$\frac{[a_{\mathrm{Mn}}]}{(a_{\mathrm{MnO}})} = K_{\mathrm{eq}} \frac{a_{\mathrm{c}}}{p_{\mathrm{CO}}}. \tag{17}$$

The standard free energy change, ΔG^{o}, for the above reaction at 1738 K is -55.80 kJ/kg-mol[6]. This yields $K_{\mathrm{eq}} \sim 1.0$ at 1738 K. Furthermore, since $(a_{\mathrm{MnO}}) = \gamma_{\mathrm{MnO}}$ (wt% MnO) and as hot metal is saturated with carbon, i.e. $[a_{\mathrm{c}}] = 1.0$, Eq. (17) is consequently simplified to:

$$\frac{(\mathrm{wt\%\,MnO})}{[\mathrm{wt\%\,Mn}]} \approx \frac{p_{\mathrm{CO}}}{\gamma_{\mathrm{MnO}}}. \tag{18}$$

For slag containing sufficient lime, activity coefficient of MnO, i.e. γ_{MnO}, can vary between 1.6 and 2.1. However, in acidic slag with CaO/SiO_2 ratio as low as 0.5, a reasonable value of γ_{MnO} appears to be 1.05 or so [10]. Similarly, off-gas composition reported in Table 1 suggests an average $p_{\mathrm{CO}} = 0.5$. Thus, to assess efficiency of ferroalloy production, the reported ratio of (%MnO)/[%Mn] (see Table 1) is compared in Fig. 4 with the corresponding $p_{\mathrm{CO}}/\gamma_{\mathrm{MnO}}$ ratio considering two different values of p_{CO}, 0.5 and 0.65, respectively.[1] The comparison suggests that the SAF, used in ferromanganese production, operates close to equilibrium and hence, production of ferromanganese can be considered as sufficiently efficient.

A comparison between predicted and actual electrical energy supply is illustrated in Fig. 5. As one would note here, the predicted energy supply has been calculated embodying calculated amount of FeMn and measured off-gas composition, respectively. As seen, actual supply of electrical energy is consistently higher than the calculated values and the extent of difference between the two is about 30%. Given the reliability of (a) thermochemical data and (b) estimated amounts of slag and hot metal, such a large discrepancy is indeed surprising. This is addressed later in the text following energy balance discussion on silicomanganese production.

Embodying amount and chemical composition of various feed materials as well as composition of hot metal and slag have earlier been shown in Table 2. Using Eqs. (1) and (11), weight of silicomanganese produced and slag generated have been estimated for each batch and compared with corresponding operating values. This is illustrated in Fig. 6. A very reasonable agreement between the two is readily evident.

A comparison between predicted and actual electrical energy requirement supply (viz., Table 2) for silicomanganese production is shown in Fig. 7. In contrast to Fig. 5, an excellent agreement (within $\pm$ 10%) between predicted and industrial data is readily evident. Close correspondence between predicted and plant data further suggests that D^{SiMn}, L and S determining collectively the electrical energy deficit vis-a-vis supply can be predicted reasonably accurately for silicomanganese production. This further implies that CO and CO_2 concentrations in the off-gas, reported in Table 2, can be taken to be reasonably representative of the actual values.

Referring back to Fig. 5, a systematic trend between predicted and operating values is readily evident; that is, predictions are consistently, about 30%, lower than the actual operating values. In contrast, difference between predicted and operating values illustrated in Fig. 7 is very reasonable. Marginal discrepancy can be attributed to uncertainties associated with various measured and thermochemical data. Referring back to Eq. (9), it is evident that under-prediction in Fig. 5 is the result of either an under-prediction of thermal demand (D) or an over-predicted energy supply (S), since energy loss (L) is shown to be a relatively small fraction of the overall thermal requirement ($\sim$ 10% or so). Since batch-wise predicted and measured amounts of ferromanganese are shown to be in reasonable agreement (e.g. Figure 3b) and chemistry of charge and product materials is fairly realistic and reproducible, possibility of a significantly under-predicted demand term (D) can be ruled out. Energy supply, on the other hand, as seen from Eq. (5), contains heat of formation of CO, CO_2 and slag (i.e.

[1] Given the discussion presented later in the text, the value of p_{co} in off-gas is somewhat uncertain. Hence, estimates, corresponding to two different possible values of p_{co} (reported to be relatively higher), are shown in Fig. 4.

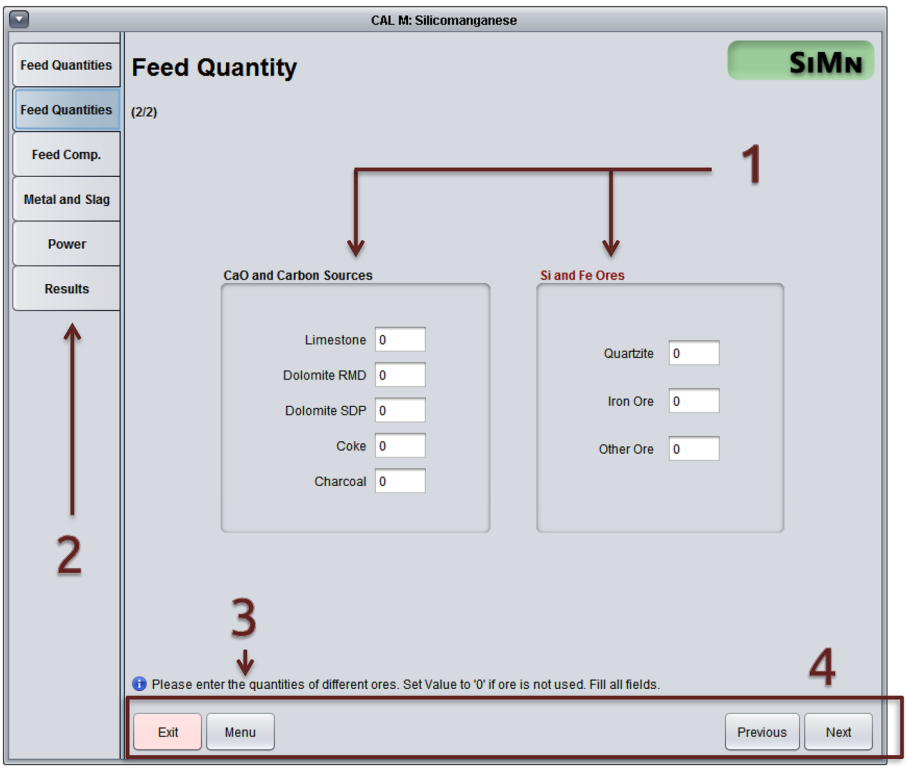

1. Data Input fields 2. Navigation tabs 3. Instructions for guidance 4. Navigational button

Fig. 2 A screenshot of a panel of the GUI developed to carry out material balance calculations

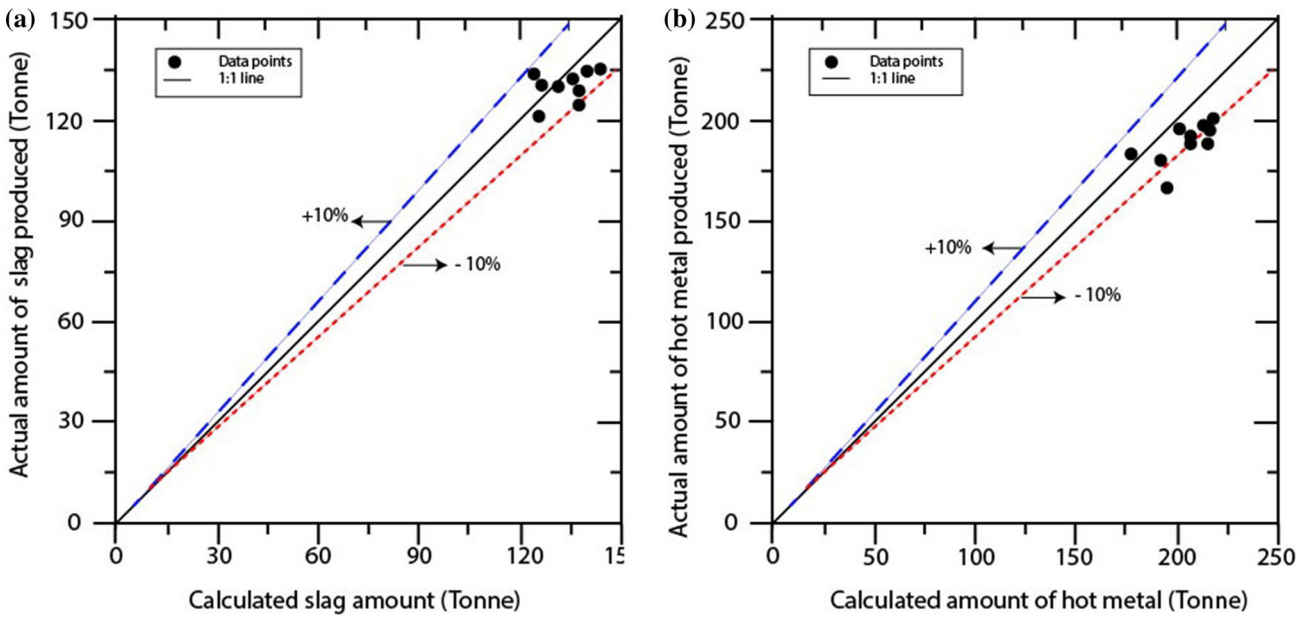

Fig. 3 Comparisons between estimated and actual amounts of **a** slag generated and **b** hot metal produced from SAF 1 during production of HCFeMn

essentially $CaO{\cdot}SiO_2$). Although the formulation of heat effect associated with slag formation has been considerably idealised in this study, inclusion of $MgO{\cdot}SiO_2$ or aluminosilicates (from their parent oxides) produces little or no changes in estimated value of 'S', since (a) moles of MgO in slag per mole of product Mn are typically small (only one-fourth of the corresponding value for CaO) and (b) *t* molar heat of formation of $MgO{\cdot}SiO_2$ is somewhat smaller than that of $CaO{\cdot}SiO_2$ [11]. The preceding discussion therefore suggests that total contributions from CO and CO_2 in the off-

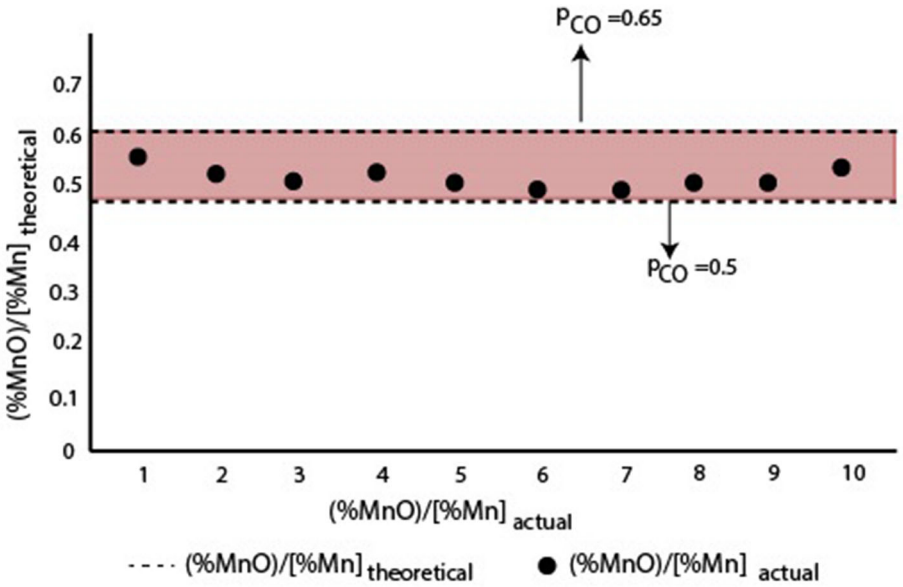

Fig. 4 A comparison of actual and equilibrium manganese partition ratio during production of high-carbon ferromanganese considering p_{CO} = 0.5 and 0.65, respectively

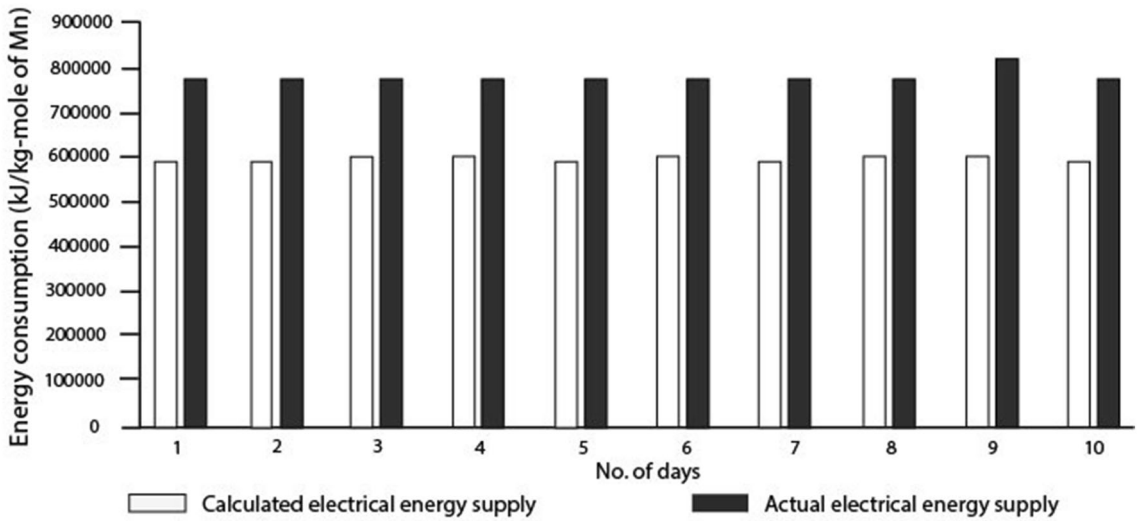

Fig. 5 Comparison between estimated and actual supply of electrical energy during production of ferromanganese in SAF 1

gas, to energy supply, warrants some careful consideration as the latter has the potential to influence energy supply, *S*, and hence the final outcome from energy balance considerations.

The molar heat of formation of CO and CO_2 at 298 K is substantially different (111,000 vs. 394,000 J/mol). Consequently, any deviation of vol % CO and CO_2 in the off-gas can introduce considerable uncertainty in energy balance calculations. It is interesting to note here that the relative proportions of CO and CO_2 in the off-gas for ferromanganese production are substantially different from those for silicomanganese production even though furnaces, materials and manufacturing processes are not drastically different. However, it is to be noted here that the proportions of CO and CO_2 in the off-gas are susceptible to change, particularly in old leaking furnaces, due to ingression of air from the surrounding. This is examined in the following from a material balance perspective for both ferromanganese and silicomanganese production.

To investigate the rather large and unexpected discrepancy between predicted and operating values shown in Fig. 5, and to concurrently examine the possibility of air ingression during ferroalloy production, oxygen balance equations have been developed and analysed. To this end, it is important to note that some oxides such as CaO, MgO, Al_2O_3 and a portion of MnO do not undergo reduction or dissociation inside submerged arc furnace. These can therefore be assumed to enter and leave the furnace as it is, exerting no influence on overall oxygen balance in SAF. Looking from such a standpoint, oxygen produced due to carbo-thermic reduction of metal oxides and calcination of fluxing agents (as CO_2) must be

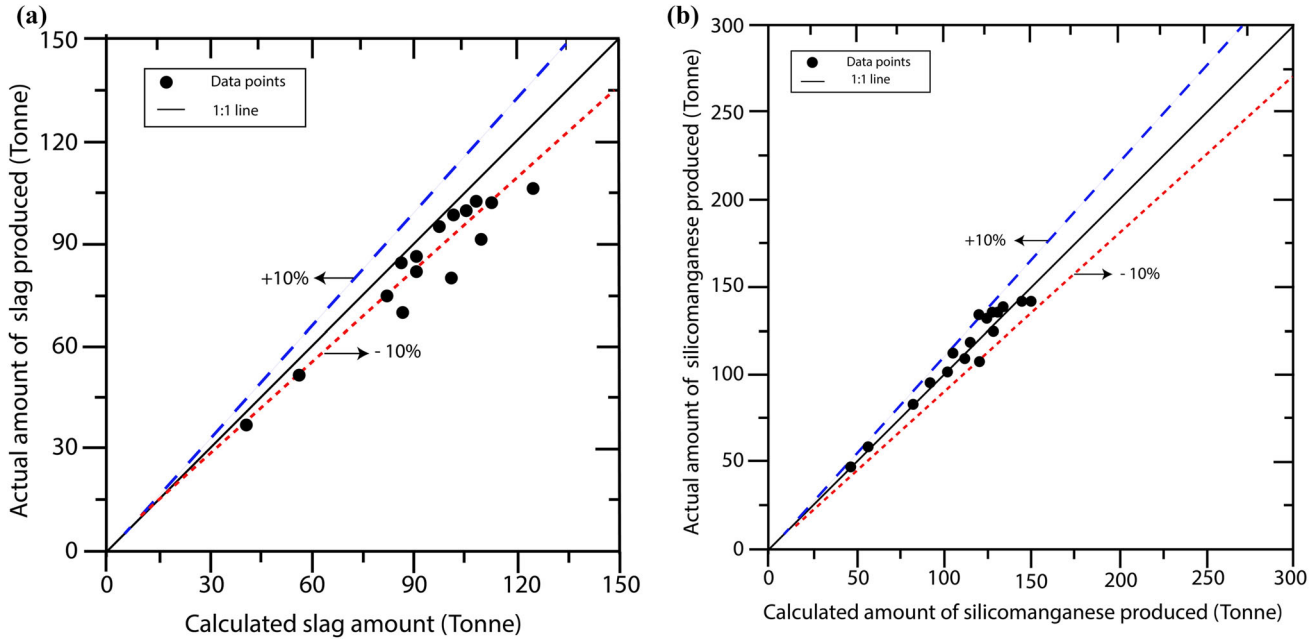

Fig. 6 Comparison between estimated and actual amount of **a** slag generated and **b** hot metal produced from SAF 2 during production of SiMn

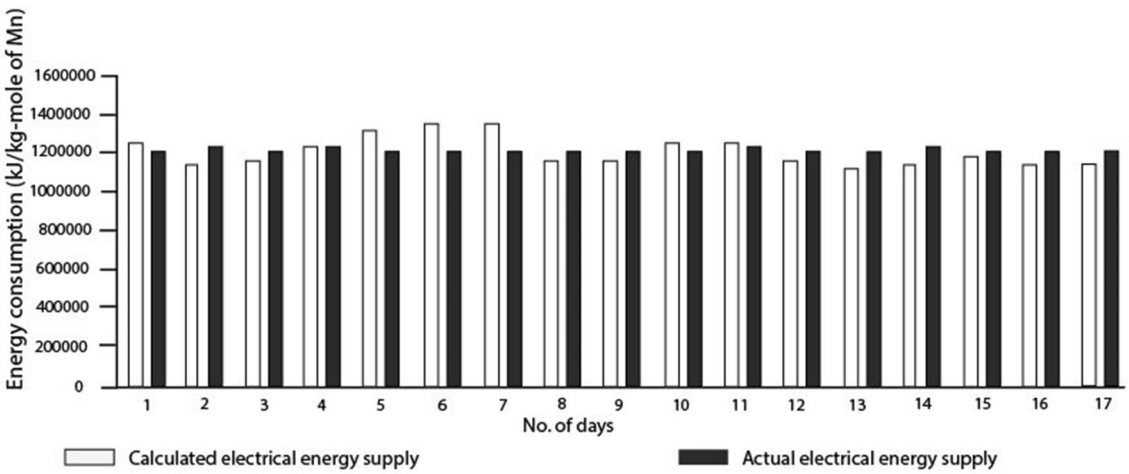

Fig. 7 A comparison between predicted and actual supply of electrical energy during production of silicomanganese

present in the off-gas, since the presence of dissolved oxygen in hot metal, in the intensely reducing environment, is unlikely. Furthermore, assuming negligible presence of FeO in the slag (e.g. Table 3), a material balance statement on oxygen can be written as:

> Moles of oxygen produced from reduction of (MnO_2 + Fe_2O_3 + SiO_2 + P_2O_5) + Moles of oxygen produced from calcination of limestone and other fluxing agents (present in combined state with carbon) = Moles of oxygen present in the off-gas as CO and CO_2.

In the above consideration, the furnace is assumed to be completely isolated and air-tight and hence, the presence of any free oxygen in the intensely reducing furnace environment has been ruled out.[2] In terms of notations used so far, the above statement can be mathematically represented as:

$$2 + 10.5(\mathrm{Fe/Mn})^{\mathrm{HM}} + 2(\mathrm{Si/Mn})^{\mathrm{HM}} + 20.5(\mathrm{P/Mn})^{\mathrm{HM}} + 2\frac{(\mathrm{wt\%\,CaO}) \times W_{\mathrm{slag}}}{56} \times \frac{1}{n_{\mathrm{Mn}}} + 2\frac{(\mathrm{wt\%\,MgO}) \times W_{\mathrm{slag}}}{40} \times \frac{1}{n_{\mathrm{Mn}}} = n_{\mathrm{C}}^{\mathrm{A}}(\mathrm{O/C})^{\mathrm{off-gas}} \quad (19)$$

[2] Exit gas analysis, in contrast, shows the presence of free oxygen in traces (see Table 1, 2).

In the above expression, $n_C^A = n_C^i - (C/Mn)^{HM} - (C/Mn)^{slag}$, where n_C^i represents kg-moles of carbon in input per kg-mole of product Mn and can be calculated from the amount of coke added, the amount of electrode paste consumed and the amount of CO_2 generated from calcination of fluxing agents (see Table 1). Therefore, given the carbon content of ferromanganese (hot metal) and slag, one can readily estimate n_C^A from an elemental carbon balance. Similarly, total moles of oxygen input (i.e. the LHS of Eq. 19) per mole of product Mn can be readily calculated, given the hot metal and slag composition as well as slag weight (known from material balance calculations). Finally, embodying reported gas composition from Table 1, $(O/C)^{off\text{-}gas}$ can also be estimated. On the basis of such, total input as well as total output of oxygen can be calculated separately and these, for some batches of ferromanganese production, are shown in Table 6(a) and (b), respectively.

It is at once evident that the difference between input and output of oxygen is significant and is negative for all the three cases, pointing out towards serious material imbalance in the process. Since input of oxygen is smaller than the corresponding output, ingression of air from the surrounding appears as a distinct possibility. In the upper part of the furnace where temperature is relatively low, air ingression can facilitate $CO \rightarrow CO_2$ conversion, resulting in higher $(O/C)^{off\text{-}gas}$. This, in turn, can amplify the energy supply term (S) in Eq. (9) producing relatively smaller estimates of $D^{FeMn} + L - S$ or $D_{ext.}^{FeMn}$, as reflected in Fig. 5. Indeed, the submerged arc furnaces considered in the present study are relatively old and hence cannot be expected to be perfectly sealed. Air ingression as well as additional heat loss (to ambient through furnace roof) consequently is not entirely unlikely. The presence of free oxygen in off-gas appears to lend support towards such supposition. Thus, if energy balance calculations are repeated considering gas composition similar to those shown in Table 2 (i.e. 71% CO and 11% CO_2 with equivalent $(O/C)^{off\text{-}gas} = 1.13$), an agreement between predicted and actual electrical energy supply is improved considerably, as illustrated in Fig. 8. However, systematic deviation between measurements and predictions, *albeit* less pronounced, still persists.

As seen from Tables 1 and 2, average off-gas temperature in SAF 1 (used for FeMn production) is considerably lower than that in SAF 2 (used for SiMn production) (i.e. average ranges are, respectively, 184–271 °C and 275–340 °C). This is consistent and is expected since relatively lower operating temperature is employed in SAF 1 for ferromanganese production. The two tables also indicate that free oxygen and CO contents in off-gas in SAF 2 are relatively higher than those in SAF 1. Thus, given higher furnace operating temperature, more air ingression in SAF 2, relative to SAF 1, may not thermodynamically facilitate $CO \rightarrow CO_2$ conversion/oxidation. Significant $CO \rightarrow CO_2$ conversion in the upper part of the furnace, as one would normally anticipate, would increase off-gas temperature due to the heat liberated from exothermic,

Table 6 An assessment of oxygen conservation during FeMn production on the basis of some data given in Table 1

Case	Moles of oxygen from manganese ore $(O/Mn)^{ore}$	Moles of oxygen from metalloid reduction			Moles of oxygen from carbonate dissociation	Total moles of oxygen per mole of manganese in input
		1.5 (Fe/Mn) (based on 23% iron by weight)	2 (Si/Mn)	2.5 (P/Mn)	2 (%CaO)·W_{Sl}/(56·n_{Mn}) + 2 (%MgO)·W_{Sl}/(40·n_{Mn})	
(a) Oxygen input						
1	2	0.48	0.016	0.022	0.291 + 0.17	2.98
2	2	0.48	0.017	0.022	0.298 + 0.177	2.99
3	2	0.48	0.017	0.022	0.323 + 0.177	3.02

Case	Exit gas composition (%)		(O/C) ratio in the carbonaceous portion of top gas	Moles of carbon per mole of manganese			Total moles of oxygen per mole of manganese in output	Input–output
				Input through coke, flux and electrode (I)	Passive carbon in metal and slag (II)	Moles of carbon in the gas phase (I–II)		
	CO	CO_2	O/C	n_C^i	$(C/Mn)^{HM} + (C/Mn)^{sl}$ (based on 6.65% C in HM and 1.5% C in slag)	n_C^A	n_C^A * (O/C)	n_O^i–n_O^o
(b) Oxygen output								
1	44	38	1.46	2.63 + 0.23 + 0.11 = 2.99	0.43 + 0.07 = 0.50	2.49	3.63	− 0.65
2	45	37	1.45	2.69 + 0.24 + 0.108 = 2.948	0.435 + 0.073 = 0.508	2.44	3.53	− 0.54
3	48	37	1.43	2.61 + 0.20 + 0.11 = 2.92	0.431 + 0.073 = 0.504	2.416	3.45	− 0.43

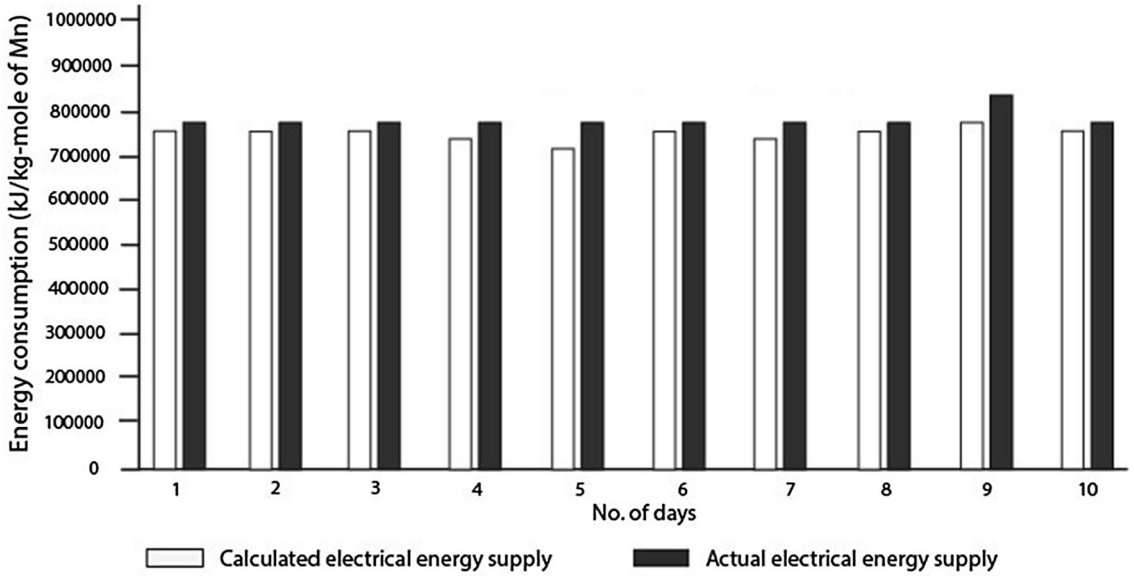

Fig. 8 A comparison between predicted and actual supply of electrical energy during production of ferromanganese in SAF 1 on the basis of a rationalised off-gas composition

oxidation reaction. However, it is not entirely unlikely that a relatively low furnace temperature coupled with substantial ingression of cold air can suppress such local temperature rise. Further, plant-scale monitoring is clearly needed to resolve the anomaly. It is interesting to note that if similar material balance calculations are carried out for silicomanganese production, oxygen imbalance is found to be less pronounced, suggesting less pronounced CO oxidation in the upper part of SAF 2. This is shown in Table 7.

As a final point, given the difficulties in conducting industrial-scale trials with rigour, day-to-day fluctuations in operating conditions and many unforeseen problems of high-temperature ferroalloy-producing units, discrepancy between prediction and measurements, to the extent shown in this work, can be considered reasonable. It is therefore

Table 7 An assessment of oxygen conservation during SiMn production for some cases from Table 2

Case	Moles of oxygen from manganese ore and recycled MnO reduction	Moles of oxygen from metalloid reduction			Moles of oxygen from carbonate dissociation	Total moles of oxygen per mole of manganese in input
	$0.82\ (O/Mn)_{MnO2} + 0.18\ (O/Mn)_{MnO}$	1.5 (Fe/Mn)	2 (Si/Mn)	2.5 (P/Mn)	$2\ (\%CaO)\cdot W_{Sl}/(56\cdot n_{Mn}) + 2\ (\%MgO)\cdot W_{Sl}/(40\cdot n_{Mn})$	
(a) Oxygen input						
1	1.82	0.48	0.99	0.02	0.376 + 0.253	3.94
2	1.82	0.48	1.0	0.025	0.37 + 0.268	3.963
3	1.82	0.48	1.05	0.025	0.397 + 0.28	4.052

Case	Exit gas composition (%)		(O/C) ratio in the carbonaceous portion of off-gas	Moles of carbon per mole of manganese			Total moles of oxygen per mole of manganese in output	Input–output
				Input through coke, coal, flux and electrode	Passive carbon in metal and slag	Moles of active carbon in the off-gas		
	CO	CO_2	O/C	n_C^i	$(C/Mn)^{HM} + (C/Mn)^{sl}$	n_C^A	$n_C^A * (O/C)$	$n_O^i – n_O^o$
(b) Oxygen output								
1	50	10	1.17	3.67	0.149 + 0.12	3.51	4.10	− 0.16
2	62	10	1.14	3.58	0.151 + 0.012	3.417	3.895	+ 0.068
3	60	14	1.19	3.69	0.151 + 0.012	3.527	4.197	− 0.145

legitimate to conclude that material and energy balance framework developed in this work is sufficiently robust and can be applied to audit and optimise ferroalloy (i.e. FeMn and SiMn) production in submerged arc furnaces.

5 Conclusions

Steady-state material and energy (enthalpy) balance expressions for ferromanganese and silicomanganese production in submerged arc furnace were developed. The adequacy of the models was assessed against data obtained from a domestic ferroalloy production unit. To this end, amount of slag and hot metal produced per batch were calculated on the basis of weight and composition of various input materials. Estimated amounts were found to be in reasonable agreement with corresponding reported values.

On the basis of material balance, appropriate enthalpy balance expressions were also formulated for the two types of ferroalloys produced in two different submerged arc furnaces. Embodying amounts of metal and slag and composition of hot metal, slag and off-gases, electrical energy required for each batch of ferroalloy produced was calculated and compared with plant data. While the prediction of external electrical energy requirement was shown to be in reasonable agreement with the supplied electrical energy for SiMn production, the same was found to be substantially different for FeMn production. To this end, air ingression into the SAF (used for manufacturing FeMn) was investigated from a material balance perspective and reported off-gas composition. Re-estimation with a rationalised off-gas composition improved the agreement between predicted and actual electrical energy supplied considerably.

References

1. Pitts A, Iron and Steel Technology, 10 (2015) p 93.
2. Batra NK, Ironmaking and Steelmaking, 30 (2003) p 399.
3. Pistorius PC, The Journal of the South African Institute of Mining and metallurgy, 2 (2002) p 33.
4. Sithole NA, Erwee MW and Steenkamp JD, 3rd Young Professionals conference, The South African Institute of Mining and Metallurgy, Pretoria (2017) p 481.
5. Olsen SE, Tansgstad M and Landstad T, *Production of Manganese Ferroalloys*, Academic Press (2007).
6. Ghosh A and Chatterjee A, *Principles and Practices in Iron and Steelmaking*, Prentice Hall, India (2008).
7. Engh TA, *Principles of Metal Refining*, Oxford Science Publication, Oxford University Press Inc., New York (1992).
8. Peacey JG and Davenport WG, *Iron Blast Furnaces: theory and Practice*, Pergamon Press (1978).
9. Mazumdar D, *A First Course in Iron and Steelmaking,* University Press, Hyderabad, India (2015).
10. Eom CH, Lee SH, Park JG, Park JH and Min DJ, ISIJ International, 56 (2016) p 37.
11. Engh TA, *Principles of Metal Refining*, Oxford Science Publications, Oxford University Press, New York (2002) p 417.